

# Spatial Normalization of Diffusion Tensor Images Based on Anisotropic Segmentation

Jinzhong Yang<sup>\*a</sup>, Dinggang Shen<sup>a</sup>, Chandan Misra<sup>a</sup>, Xiaoying Wu<sup>a</sup>,  
Susan Resnick<sup>b</sup>, Christos Davatzikos<sup>a</sup>, and Ragini Verma<sup>†a</sup>

<sup>a</sup>Section of Biomedical Image Analysis, Department of Radiology,  
University of Pennsylvania School of Medicine, Philadelphia, PA USA 19104;

<sup>b</sup>Laboratory of Personality and Cognition, NIA, Baltimore, MD USA 21224

## ABSTRACT

A comprehensive framework is proposed for the spatial normalization of diffusion tensor (DT) brain images using tensor-derived tissue attributes. In this framework, the brain tissues are first classified into three categories: the white matter (WM), the gray matter (GM), and the cerebral-spinal fluid (CSF) using the anisotropy and diffusivity information derived from the full tensor. The tissue attributes obtained from this anisotropic segmentation are then incorporated into a very-high-dimensional elastic registration method to produce a spatial deformation field. Finally, the rotational component in the deformation field, together with the estimated underlying fiber direction, is used to determine an appropriate tensor reorientation. This framework has been assessed quantitatively and qualitatively based on a sequence of experiments. A simulated experiment has been performed to evaluate the accuracy of the spatial warping by examining the variation between deformation fields. To verify the tensor reorientation, especially, in the anisotropic microstructures of WM fiber tissues, an experiment has been designed to compare the fiber tracts generated from the DT template and the normalized DT subjects in some regions of interest (ROIs). Finally, this method has been applied to spatially normalize 31 subjects to a common space, the case in which there exist large deformations between subjects and the existing approaches are normally difficult to achieve satisfactory results. The average across the individual normalized DT images shows a significant improvement in signal-to-noise ratio (SNR).

**Keywords:** Diffusion tensor imaging, registration, anisotropic segmentation

## 1. INTRODUCTION

Diffusion tensor imaging (DTI) is a magnetic resonance (MR) imaging modality which is able to measure water diffusivity in tissue non-invasively<sup>1</sup>. It has been observed that water diffusivity is more restricted in the transverse direction of the axonal fibers in white matter tissue than along the axial direction of the fibers. DTI takes advantage of this anisotropic diffusion of the water molecules and measures a symmetric second order tensor at each voxel to characterize the anisotropy. The principal direction (PD) of the tensor is presumed to coincide with the underlying fiber orientation. Therefore, DTI can provide unique micro-structural and physiological information insight into the white matter of brains, which has not been found available in other MR modalities, and has thus become a powerful technique for analyzing the underlying white matter structure of brains<sup>2,3</sup>. The rich micro-structural information of white matter facilitates the study of development, aging, and disease on specific white matter regions of interest.

In clinical studies, for example, in the study of group difference between patients and healthy controls, it is very important to remove the inter-individual morphological variability in order to make subjects comparable. This is achieved by spatially normalizing all subjects to a common template. Subsequent analysis can be carried out using these normalized images. However, spatial normalization of diffusion tensor images is rendered challenging by the fact that the data representation is high dimensional and it requires not only the spatial warping, but also the tensor reorientation at each voxel<sup>4-6</sup>. Therefore, deformable registration methods developed for scalar images may not be directly applicable to the tensor data. Several diffusion tensor registration methods have been proposed in the literature. Some earlier work registered the tensor data using scalar maps derived from diffusion tensor (DT) images without considering the tensor

---

\*Email: jinzhong.yang@uphs.upenn.edu; phone: (215) 662-3110. †Email: ragani.verma@uphs.upenn.edu; phone: (215) 662-7471.

reorientation<sup>7-9</sup>. Park et al.<sup>10</sup> proposed a registration method by using multiple channels generated from the tensor image, but the tensor orientation was not explicitly considered for optimization. Goh and Vidal<sup>11</sup> presented an algebraic methods for DTI registration, but this method deals with only affine transformation. Zhang et al.<sup>6</sup> applied a piecewise affine transform for the deformable registration of diffusion tensors, while their method is limited to small deformation. Cao et al.<sup>12</sup> proposed a diffeomorphic matching of DT images, which is promising for large deformation. However, the complicated energy function might suffer from local optima during optimization.

Existing methods of spatial normalization for tensor data have revealed that it is insufficient to consider only the scalar maps of anisotropy for registration as it is unable to correctly align the tensor orientation. It is also not acceptable to use the context from the corresponding structural images since they are difficult to align with the tensor images due to distortions. Further, using the full tensor information without the explicit context of anisotropy and diffusivity may not produce sufficient feature information to yield a robust tensor registration. Therefore, we have been motivated to develop a framework, which integrates the tensor-derived anisotropy and diffusivity information to define tissue attributes to drive a deformable registration for the tensor images. The proposed framework has been successfully applied to spatially normalize both human brain DT images and mouse brain DT images. The accuracy and robustness of this spatial normalization method are assessed qualitatively and quantitatively using both simulated and real data. We also demonstrate the applicability of our method in handling data sets with large deformation around the ventricles, the case in which most existing approaches are normally unable to achieve satisfactory results.

## 2. METHODS

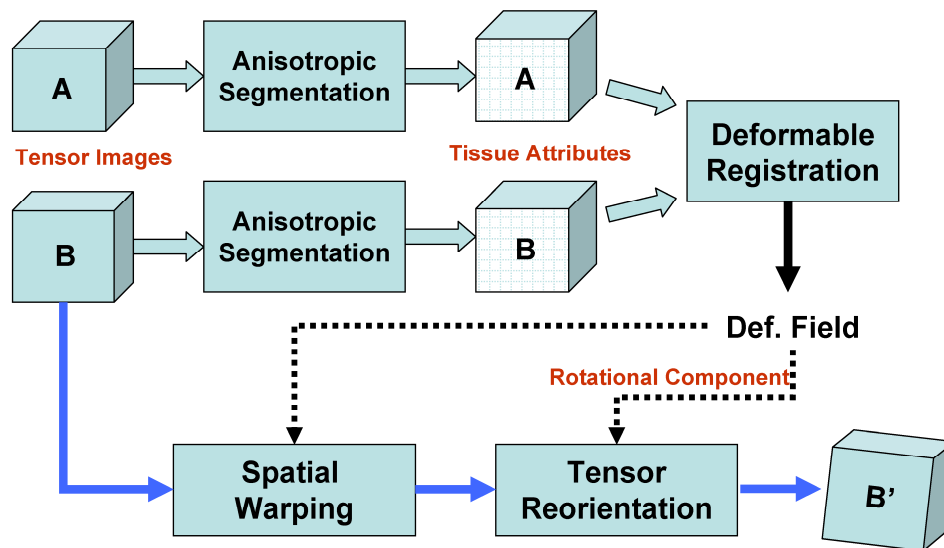


Fig. 1. Spatial normalization framework for the diffusion tensor images. The subject image **B** is deformed to image **B'**, which resides in the template space of image **A**.

The proposed deformable registration method for DT images incorporates the tensor-derived tissue attributes into a very high-dimensional elastic registration method<sup>13</sup> followed by a tensor reorientation scheme that employs tensor information retrieved from adaptively selected regions<sup>5</sup>. The overall framework of this method is illustrated in Fig. 1. It mainly consists of three steps. Firstly, the brain tissues of template image **A** and the subject image **B** are roughly classified into three categories: white matter (WM), gray matter (GM), and cerebral-spinal fluid (CSF), by employing anisotropic segmentation on fractional anisotropy (FA) and apparent diffusion coefficient (ADC) maps derived from the DT image. The anisotropic segmentation estimates a fuzzy map of WM and a fuzzy map of CSF from the FA and the CSF respectively using fuzzy C-Means algorithm, and then produces tissue attributes of WM, GM, and CSF from the fuzzy WM and CSF maps using the K-Means algorithm. The tissue attributes are incorporated into a deformable registration algorithm, named *hierarchical attribute matching mechanism for elastic registration* (HAMMER)<sup>13</sup>, to

generate a deformation field that characterizes the spatial deformation from the template image to the subject image. Finally, the deformation field is applied to spatially warp the subject image, and the rotational component extracted from the deformation field, together with the estimated underlying fiber directions, is used to determine an appropriate tensor reorientation<sup>5</sup>, thus producing the spatially normalized image  $\mathbf{B}'$ .

## 2.1 Anisotropic Segmentation

Anisotropic segmentation provides salient and unique tissue attributes for the spatial normalization of diffusion tensors. The boundaries between different tissues give rich information for well aligning brain images. More robust registration could be expected by using the tissue attributes than using the intensity images. Direct segmentation on diffusion tensors is difficult due to the high dimensional data representation, while most traditional segmentation methods are normally based on the scalar structural images. Further, none of the tensor-derived measures of anisotropy and diffusivity can individually provide tissue attributes specific enough to drive the registration; therefore, it requires a combination of information from different tensor derived measures. For registration purpose, brain tissues are normally separated into three categories, i.e. WM, GM, and CSF. A simple method performs segmentation for diffusion tensor images by setting two thresholds on a joint space of the FA and ADC maps<sup>3</sup>. However, this method is not generalizable to different data sets as it is based on setting a very specific threshold and it is vulnerable to noise. Another method attempts to perform segmentation using multiple overlapped tensor-derived scalar measures as well as including the anatomical information from the  $T_2$ -weighted image<sup>14</sup>; however, in concern of the increasing complexity, the overlapped scalar measures might not be necessary when the segmentation is for the purpose of registration. Therefore, we propose the anisotropic segmentation, which combines anisotropic and diffusivity information contained in the FA and ADC measures, to generate tissue attributes for the spatial normalization.

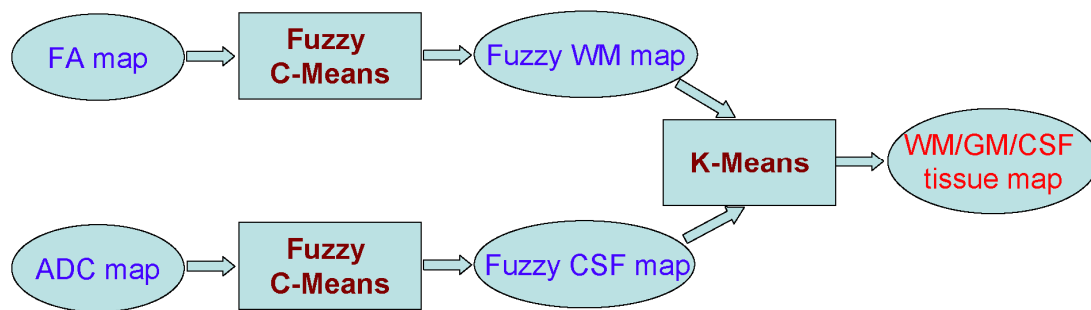


Fig. 2. Anisotropic segmentation for diffusion tensor images. The FA and ADC scalar maps derived from the DT image are used to generate tissue attributes with WM, GM, and CSF.

Fig. 2 illustrates the anisotropic segmentation based on the tensor-derived FA and ADC measures. Owing to the inherently anisotropic feature of WM, one is able to roughly separate WM and non-WM tissues from the FA map. Similarly, the coefficients of CSF in the ADC map are much larger than those of other tissues, so that CSF and non-CSF tissues can be roughly separated. Instead of directly segmenting the FA map into a binary WM/non-WM tissue map, we estimate a fuzzy WM map  $\mathbf{x}$  by applying the fuzzy C-Means algorithm<sup>15,16</sup> to the FA map. Each voxel on this fuzzy map takes values from the interval  $[0, 1]$ , which implies the probability of a voxel belonging to the WM tissue. With the algorithm in<sup>16</sup>, one can adjust a smoothness factor to mitigate the adverse effect from noise. Similarly, a fuzzy CSF map  $\mathbf{y}$  is estimated from the ADC map. Finally, we combine these two fuzzy maps to formulate a feature vector  $(x_i, y_i)$  for each voxel at location  $i$ , and feed the feature vector into a K-Means classifier to generate a tissue map with tissue attributes of WM, GM, and CSF. With the prior knowledge we can initialize the class centers as follows:

$$\begin{cases} (1.0, 0.0) : \text{the initial center for WM tissue} \\ (0.0, 1.0) : \text{the initial center for CSF tissue} \\ (0.0, 0.0) : \text{the initial center for GM tissue} \end{cases}$$

This anisotropic segmentation has been demonstrated to be efficient and robust. The results are consistent across individual subjects that we have studied. Our experiments also demonstrate that the produced tissue attributes are good enough to drive the subsequent spatial normalization.

## 2.2 Deformable Registration

The deformable registration for scalar images has been actively investigated for decades<sup>13,17-19</sup>. In the proposed framework we incorporate the tensor-derived tissue attributes into a high-dimensional elastic registration approach, which is referred to as HAMMER<sup>13</sup>, for the spatial normalization of DT images. This approach was developed for registering  $T_1$ -weighted brain images, with the tissue maps of WM, GM, and CSF being the inputs. Since we are able to segment the DT image into these three tissue types, this method can be extended to register DT images. This approach uses an attribute vector, which is defined on each voxel in an image and is computed from the tissue maps, to determine point correspondences between a subject and a template. The template resides in the stereotaxic space and all subjects are warped to this space. This framework relies on a hierarchical structure to select distinct attribute vectors, thus reducing ambiguity in finding correspondences. Relatively fewer and more stable attributes are selected in the initial stages of the matching procedure to help avoid local minima, a known problem in high-dimensional computation. Finally, the hierarchical sequence of piecewise smooth transformations are concatenated to result in a spatial transformation from the template to the subject. The readers are referred to<sup>13</sup> for details of this algorithm.

## 2.3 Tensor Reorientation

The spatial warping by relocating the tensors in a DT image should ideally remove most variability in isotropic anatomies, e.g. the GM tissue. However, the variability in anisotropic anatomies, e.g. the WM tissue, still exists since the orientation and thickness of WM fiber tracts are still different. Therefore, it requires performing tensor reorientation after the spatial warping. It is also crucial to note the following two points when performing tensor reorientation. First, the same spatial transformation could have different rotation effects on differently oriented tensors, which implies that one can not directly apply the rotational component of the spatial transformation to reorient the tensors. To properly reorient the tensors, one must consider the underlying fiber orientation. Second, the shape of tensors must be preserved during tensor reorientation. The shape of tensors reveals the local tissue microstructure, which is presumed unchanged during DT warping. Two reorientation strategies were proposed in<sup>4</sup>. One is the finite strain (FS), which extracts a rotational component from the entire deformation field and applies it to rotate the diffusion tensors at each voxel. The drawback of this strategy is that it discards the local deformation that affects the tensor orientation, and it does not consider the underlying tensor orientation. Another strategy is the preservation of principal direction (PPD), which estimates the rotational component for each voxel based on the deformation and the underlying principal direction at this voxel. This strategy is vulnerable to noise since it estimates the rotational component from only the tensor information at current voxel. To better perform the tensor reorientation, we adopt the approach presented in<sup>5</sup>. This approach determines an appropriate tensor reorientation for each voxel from a neighborhood region. The direction of the underlying fiber at each voxel is assumed to follow a probability distribution, which is estimated by treating the principal eigenvectors in the neighborhood region as random samples drawn from the distribution. The shape of the neighborhood is adaptively chosen to avoid the inclusion of tensors from isotropic tissues adjacent to the fiber. The details of this approach can be found in<sup>5</sup>.

# 3. RESULTS

## 3.1 Datasets

*Human brain data:* The human brain data were acquired as part of the Baltimore Longitudinal Study of Aging (BLSA) study. 31 subjects were selected from both genders and with ages ranging from 56 to 94. The images were acquired using 1.5T Philips scanner. Each of the dataset consisted of 30 gradient directions with the diffusion weighting of  $b=700$  s/mm<sup>2</sup> (NEX = 2). The imaging dimension was 256×256 with a rectangular field of view (FOV) as 240×240. The slice thickness was 2.5 mm without a gap, and 50 slices covered the entire brain. The DTI data reconstruction was performed in DTI Studio<sup>20</sup>, and the scalar maps of FA and ADC were also generated by this tool. The reconstructed DTI data were then zero-padded to the size of 256×256×70 with the data resolution as 0.9375×0.9375×2.5 mm. All of the DTI data, as well as the derived scalar maps, were skull-stripped using a semi-manual method before they were applied to the study.

*Mouse brain data:* Images of inbred mice of the C57BL/6J strain at different development stages were used for the study. The images were acquired using a 9.4 T Bruker scanner equipped with triple-axis gradients, and Bruker commercial volume coils (10mm to 25mm inner diameter) as dual purpose radio-frequency transmitter and receiver. Three-dimensional multiple spin echo sequence was used to acquire diffusion weighted image. The length of the

multiple spin echo train is 6. Within each TR, 6 echoes were used to acquire the k-space data for a 3D volume image. Parameters for the diffusion-weighted imaging were: FOV=8-16/8-10/8-10mm, 3D imaging matrix = 128×80×80 (zero-filled to 128×128×128), TE=34ms, TR=800ms, 6 independent directions with  $b = 1000 \text{ s/mm}^2$ , and 2 additional images with a minimal diffusion weighting ( $b= 50 \text{ s/mm}^2$ ). Native image resolutions ranged from 62.5×100×100  $\mu\text{m}$  to 125×125×125  $\mu\text{m}$ . Two signal averages were used. The images were further averaged from 6 echoes of each repetition time. The DTI reconstruction and processing were the same as described for the human brain data.

### 3.2 Simulation

We designed a simulation to evaluate the accuracy of the proposed registration method. One healthy human brain was chosen randomly from the BLSA database as the template. We applied ten simulated deformation fields to produce ten simulated diffusion tensor subjects. The simulated deformation fields, which serve as the ground truth in the simulation, are generated using the statistical model of deformation (SMD) in <sup>21</sup> by training a set of deformation fields obtained from registering real MR images. These ten simulated deformation fields are very different so that the variability across different subjects is taken into account. These ten simulated subjects were registered back to the template space using our proposed method. The difference between the reconstructed deformation fields and the corresponding ground truth is used as a measurement to evaluate the accuracy of registration. Assume the volume size is  $V$ ,  $\Delta\mathbf{s}_i = [\Delta x_{si}, \Delta y_{si}, \Delta z_{si}]^T$  the deformation vector at location  $i$  of the ground truth deformation field, and  $\Delta\mathbf{t}_i = [\Delta x_{ti}, \Delta y_{ti}, \Delta z_{ti}]^T$  the deformation vector at location  $i$  of the reconstructed deformation field. Then the registration error is evaluated by the average difference  $\bar{m}_d$  of two deformation fields and the standard deviation (SD) of the difference  $\sigma_d$  as

$$\bar{m}_d = \frac{1}{V} \sum_{i=1}^V \|\Delta\mathbf{s}_i - \Delta\mathbf{t}_i\|, \quad \sigma_d = \sqrt{\frac{1}{V} \sum_{i=1}^V (\|\Delta\mathbf{s}_i - \Delta\mathbf{t}_i\| - \bar{m}_d)^2}. \quad (1)$$

The registration error and the SD of the error for these ten simulated subjects are computed and shown in Fig. 3. It can be observed that the registration error is very small, varying from 0.79 to 0.92 voxels. The population mean of the error is 0.86 voxels. Although the ten simulated brains have great variability, the registration errors across the ten simulations are consistently small. This demonstrates that our method achieves good spatial normalization.

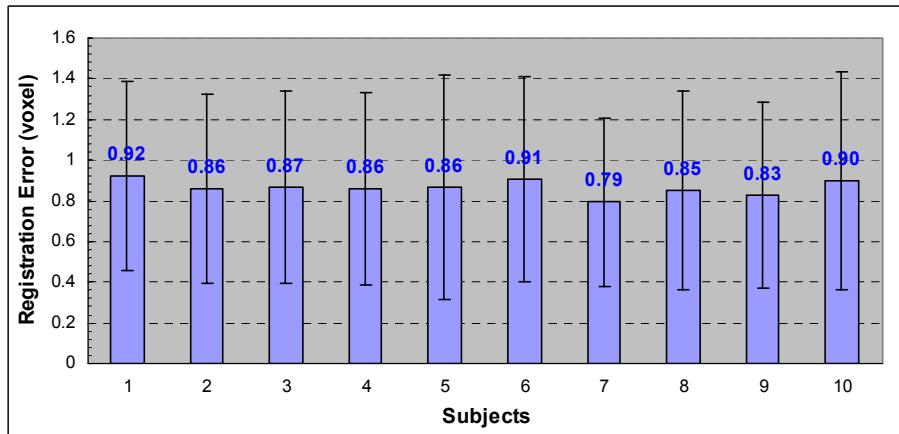


Fig. 3. Averaged registration errors for 10 simulated subjects. Error bar is the standard deviation of the registration error.

### 3.3 Tractography

Fiber tractography is applied to evaluate the accuracy of spatial normalization for diffusion tensors in this paper. In order to assess the spatial normalization of diffusion tensors, we generate the fiber tracts on the template DT image, individual warped DT images, and the normalized group-averaged DT image, respectively, using a deterministic streamline tractography method known as FACT<sup>22,23</sup>. By comparing the similarity of fiber tract bundles passing through some regions of interest (ROIs) between the subject and the template, we are able to quantify how well the spatial normalization works in these specific ROIs. Nine healthy subjects were picked from the BLSA database and we normalized eight subjects to the ninth one that is regarded as the template using our proposed registration method. An average DT image was calculated from the eight warped DT images by voxel-wise averaging the corresponding

components of the corresponding tensors. We then performed fiber tracking on the template, the individual warped subjects, and the group averaged image. The fiber tracking was performed in DTI Studio<sup>20</sup>, with an FA threshold 0.25 to start tracking, and an FA threshold 0.2 or a turning angle 70° to stop tracking. We extracted the fiber bundles for examination using two ROIs, which resides in the genu and the body of the corpus callosum (CC). Fig. 4 illustrates two fiber bundles extracted from the template image using these two ROIs.

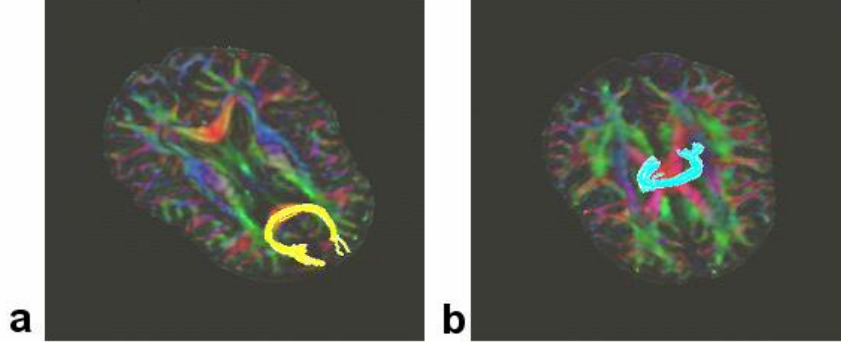


Fig. 4. Fiber bundles extracted using two ROIs in CC from the template image. **a**: ROI in the genu of CC; **b**: ROI in the body of CC.

To quantitatively assess the similarity of two fiber bundles, we computed the fiber bundle distance using the mean of the closest distances, similar to the measurement used in <sup>6</sup>. To be specific, let  $d(\cdot, \cdot)$  be a pairwise distance between two fibers, the distance between two fiber bundles  $F$  and  $G$  is defined as

$$\bar{d} = \frac{1}{|F| + |G|} \left( \sum_{F_i \in F} \min_{G_j \in G} d(F_i, G_j) + \sum_{G_j \in G} \min_{F_i \in F} d(F_i, G_j) \right), \quad (2)$$

where  $|F|$  and  $|G|$  are the number of fibers in the two fiber bundles respectively,  $\min_{G_j \in G} d(F_i, G_j)$  is the distance between the fiber  $F_i$  and the closest fiber in  $G$ , and  $\min_{F_i \in F} d(F_i, G_j)$  is the distance between the fiber  $G_j$  and the closest fiber in  $F$ . The pairwise distance between two fibers,  $d(\cdot, \cdot)$ , is defined as the mean of the closest distance for every point of two fibers, like the one defined in <sup>24</sup>. For two identical fiber bundles being perfectly registered, the distance  $\bar{d}$  becomes zero. Fig. 5 shows the fiber bundle distances between the warped subjects and the template. The ninth subject in Fig. 5 denotes the group-averaged image. The small distance between fiber bundles demonstrates a good registration of the diffusion tensor images. We also find that the distance between the group averaged image and the template is much smaller than the distances between the individual warped subjects and the template. This shows that the group-averaged image can remove the spurious fiber tracts detected in the individual warped subjects.

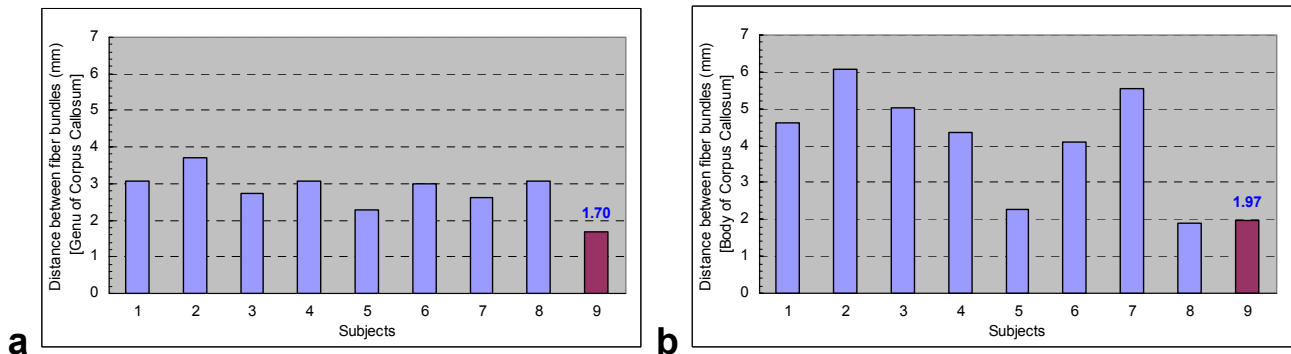


Fig. 5. The distance of the fiber bundles between each of the eight individual warped subjects and the template. The Subject 9 denotes the group-averaged image.

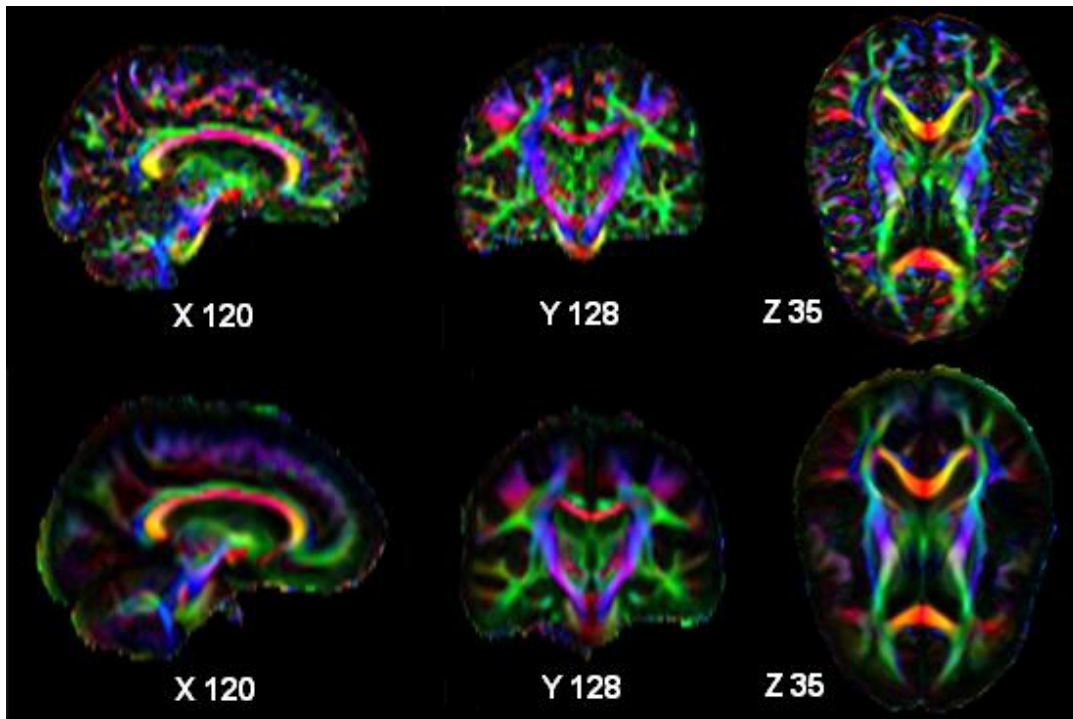


Fig. 6. Color map of the principal direction of the template human brain (first row) and the group-averaged human brain (second row) in typical sagittal, coronal, and axial views.

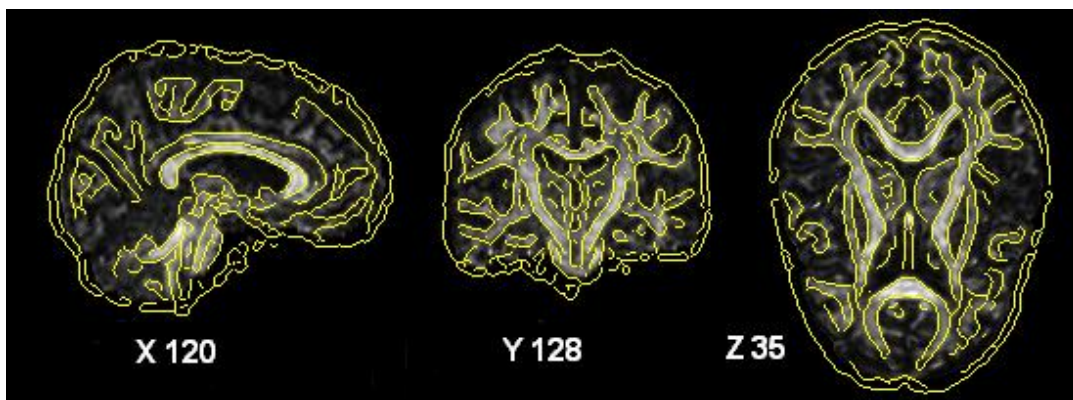


Fig. 7. Edge maps extracted from the group-averaged FA image of human brains superimposed on the template FA image in typical sagittal, coronal, and axial views.

### 3.4 Normalization of human brain DT images

We applied our method to the study of human brains. 31 subjects with both genders and of different ages have been selected from the BLSA database for this study. There exist large deformations in the ventricle among these 31 subjects, which is normal for brains in the range of these ages. We first identify one subject as the template, and then normalize the other 30 subjects to the template space by the proposed registration framework. A group averaged DT image is computed by voxel-wise averaging the corresponding tensors in the individual warped DT images. Fig. 6 shows three typical slices in sagittal, coronal, and axial views of the color-coded PD for the template and the group-averaged DT images, respectively. The PD of the tensors is weighted by the corresponding FA value so that the isotropic anatomies are suppressed from showing on the color map. The color is encoded with green representing anterior-posterior, blue for feet-head, and red for left-right orientation. By comparing the group-averaged color map with the individual template color map, we can see that the major fibers are well aligned after the spatial normalization. The group-averaging also removes most of the noise so as to highlight the major fibers, which is beneficial to subsequent group analysis and

clinical studies on WM microstructures. Subsequent analysis on the group-averaged image may also produce an atlas for the major WM structures in human brain.

To demonstrate the accuracy of the spatial normalization, we extracted the edges of group-averaged FA image and superimposed them on the corresponding template FA image for verification. Fig. 7 shows the typical views of the edge map corresponding to the color map in Fig. 6. The edge map shows a good consistency between the group-averaged FA image and the template FA image inside the brain, especially on the major WM fiber tracts, which on the other hand demonstrates a good registration. The edge map also shows the robustness of the proposed registration method in handling different subjects. If the warped images from different subjects are not consistent, the group-averaging will blur the inconsistent parts so that the existing edges can not be detected. Fig. 7 shows that most edges in the template have corresponding edges detected in the group-averaged image, which demonstrates the robustness.

### 3.5 Normalization of mouse brain DT images

We also applied our registration method to spatially normalize postnatal mouse brains. These mouse brains were acquired as part of the project to create a normative atlas of the developing mouse brains, thus requiring the spatial normalization of them in different development stages<sup>25</sup>. In this study, we randomly selected six mice with 3 males and 3 females from days 7, 10, 15, 20, 30, and 40, and normalized them to a mouse on day 10. A group averaged DT is computed by voxel-wise averaging the corresponding tensors in the individual warped mouse brain images. Fig. 8 shows three typical slices in sagittal, coronal, and axial views of the color-coded PD for the template and the group-averaged DT images, respectively. The color code is the same as that described in the experiment of normalizing human brain images. By comparing the sharpness of the group-averaged color map with the individual template color map, we can see that a good spatial normalization has been achieved and even the thin tracts like internal and external capsules have been aligned well. The good registration will lead to a good normative atlas of the developing mouse brains.

To further demonstrate the accuracy of the spatial normalization on mouse brains, we again extracted the edges of group-averaged FA image and superimposed them on the corresponding template FA image. Some typical views of the edge map are shown in Fig. 9. The edge map shows that most edges in the template have corresponding edges detected in the group-averaged image, which demonstrates the accuracy and robustness of the registration method. We did notice some inconsistency around the boundary, especially on the sagittal view; this is due to unclean separation of the skull from the brain.

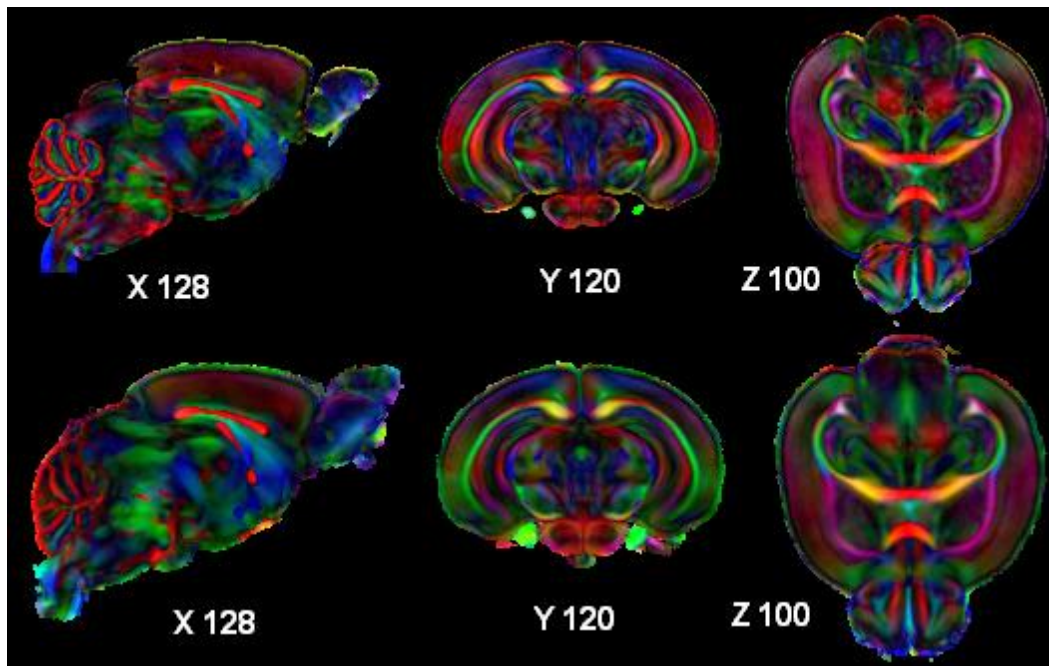


Fig. 8. Color map of the principal direction of the template mouse brain (first row) and the group-averaged mouse brain (second row) in typical sagittal, coronal, and axial views.

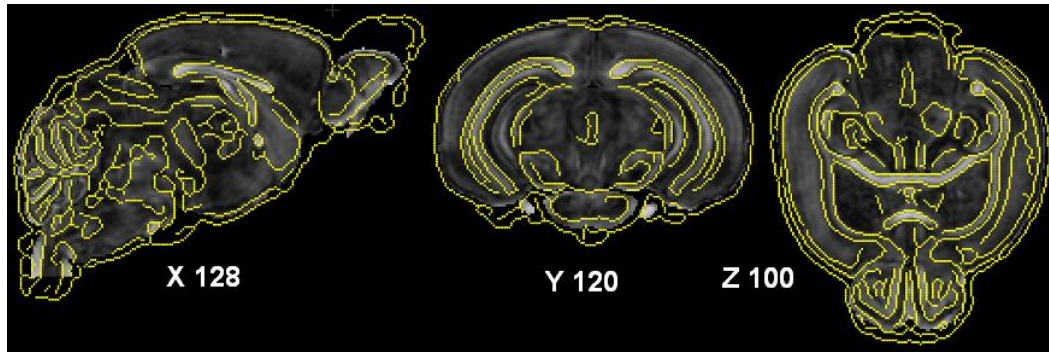


Fig. 9. Edge maps extracted from the group-averaged FA image of mouse brains superimposed on the template FA image in typical sagittal, coronal, and axial views.

#### 4. CONCLUSION

In conclusion, we have presented a comprehensive registration framework for the spatial normalization of diffusion tensor images. This framework classified the brain tissues into three categories: WM, GM, and CSF, based on the tensor-derived anisotropy and diffusivity measures. By incorporating these tensor-derived tissue attributes into a sophisticated deformable registration algorithm, followed by appropriate tensor reorientation, we obtained a robust method for the spatial normalization of DT images. The extensive experimentation on human and mouse brain data sets demonstrated the accuracy, robustness, and applicability of our proposed registration framework.

#### 5. ACKNOWLEDGEMENTS

The work in this paper was supported by the NIH grant MH070365. The aging data used in this paper were acquired as part of the Neuroimaging Study of the Baltimore Longitudinal Study of Aging (BLSA). The BLSA neuroimaging study is supported by N01-AG-3-2124 and the Intramural Research Program, National Institute on Aging, NIH.

#### REFERENCES

- [1] Basser, P. J., Mattiello, J., and LeBihan, D., "Estimation of the effective self-diffusion tensor from the NMR spin echo," *Journal of Magnetic Resonance, Series B* 103 (3), 247-54 (1994).
- [2] Mori, S., Itoh, R., Zhang, J., Kaufmann, W. E., Van Zijl, P. C. M., Solaiyappan, M., and Yarowsky, P., "Diffusion tensor imaging of the developing mouse brain," *Magnetic Resonance in Medicine* 46 (1), 18-23 (2001).
- [3] Pierpaoli, C., Jezzard, P., Basser, P. J., Barnett, A., and Chiro, G. D., "Diffusion tensor MR imaging of human brain," *Radiology* 201 (3), 637-648 (1996).
- [4] Alexander, D. C., Pierpaoli, C., Basser, P. J., and Gee, J. C., "Spatial transformations of diffusion tensor magnetic resonance images," *IEEE Transactions on Medical Imaging* 20 (11), 1131-1139 (2001).
- [5] Xu, D., Mori, S., Shen, D., Zijl, P. C. M. v., and Davatzikos, C., "Spatial Normalization of Diffusion Tensor Fields," *Magnetic Resonance in Medicine* 50 (1), 175-182 (2003).
- [6] Zhang, H., Yushkevich, P. A., Alexander, D. C., and Gee, J. C., "Deformable registration of diffusion tensor MR images with explicit orientation optimization," *Medical Image Analysis* 10 (5), 764-785 (2006).
- [7] Ruiz-Alzola, J., Westin, C. F., Warfield, S. K., Alberola, C., Maier, S., and Kikinis, R., "Nonrigid registration of 3D tensor medical data," *Medical Image Analysis* 6 (2), 143-161 (2002).
- [8] Jones, D. K., Griffin, L. D., Alexander, D. C., Catani, M., Horsfield, M. A., Howard, R., and Williams, S. C. R., "Spatial normalization and averaging of diffusion tensor MRI data sets," *Neuroimage* 17, 592-617 (2002).
- [9] Guimond, A., Gutmman, C. R. G., Warfield, S. K., and Westin, C.-F., "Deformable registration of DT-MRI data based on transformation invariant tensor characteristics," *ISBI*, (2002).

- [10] Park, H. J., Kubicki, M., Shenton, M. E., Guimond, A., McCarley, R. W., Maier, S. E., Kikinis, R., Jolesz, F. A., and Westin, C.-F., "Spatial Normalization of Diffusion Tensor MRI Using Multiple Channels," *Neuroimage* 20 (4), 1995-2009 (2003).
- [11] Goh, A. and Vidal, R., "Algebraic Methods for Direct and Feature Based Registration of Diffusion Tensor Images," *ECCV*, Leonardis, A., Bischof, H., and Pinz, A., 514-525 (2006).
- [12] Cao, Y., Miller, M., Mori, S., Winslow, R. L., and Younes, L., "Diffeomorphic matching of diffusion tensor images," *MMBIA*, New York, NY, 67 (2006).
- [13] Shen, D. and Davatzikos, C., "HAMMER: Hierarchical attribute matching mechanism for elastic registration," *IEEE Trans. on Med. Imag.* 21 (11), 1421-1439 (2002).
- [14] Liu, T., Li, H., Wong, K., Tarokh, A., Guo, L., and Wong, S. T. C., "Brain tissue segmentation based on DTI data," *NeuroImage* 38, 114-123 (2007).
- [15] Bezdek, J., Ehrlich, R., and Full, W., "FCM: Fuzzy C-Means Clustering Algorithm," *Computers & Geosciences* 10 (2-3), 191-203 (1984).
- [16] Pham, D. L., "Spatial Models for Fuzzy Clustering," *Computer Vision and Image Understanding* 84 (2), 285-297 (2001).
- [17] Gee, J. C., Reivich, M., and Bajcsy, R., "Elastically deforming 3D atlas to match anatomical brain images," *Journal of Computer Assisted Tomography* 17, 225-236 (1993).
- [18] Christensen, G. E. and Johnson, H. J., "Consistent Image Registration," *IEEE Transactions on Medical Imaging* 20 (7), 568-582 (2001).
- [19] Davatzikos, C., "Spatial transformation and registration of brain images using elastically deformable models," *Computer Vision and Image Understanding* 66 (2), 207-222 (1997).
- [20] Jiang, H., Van Zijl, P. C., Kim, J., Pearlson, G. D., and Mori, S., "DtiStudio: resource program for diffusion tensor computation and fiber bundle tracking.," *Computer Methods and Programs in Biomedicine* 81 (2), 106-116 (2006).
- [21] Xue, Z., Shen, D., Karacali, B., Stern, J., Rottenberg, D., and Davatzikos, C., "Simulating deformations of MR brain images for validation of atlas-based segmentation and registration algorithms," *NeuroImage* 33 (3), 855-866 (2006).
- [22] Mori, S., Crain, B. J., Chacko, V. P., and van Zijl, P. C., "Three-dimensional tracking of axonal projections in the brain by magnetic resonance imaging," *Annals of Neurology* 47 (2), 265-269 (1999).
- [23] Xue, R., van Zijl, P. C. M., Crain, B. J., Solaiyappan, M., and Mori, S., "In vivo three-dimensional reconstruction of rat brain axonal projections by diffusion tensor imaging," *Magnetic Resonance in Medicine* 42 (6), 1123-1127 (1999).
- [24] Gerig, G., Gouttard, S., and Corouge, I., "Analysis of brain white matter via fiber tract modeling," *EMBS*, San Francisco, CA, USA, 4421-4424 (2004).
- [25] Verma, R., Mori, S., Shen, D., Yarowsky, P., and Davatzikos, C., "Spatio-temporal maturation patterns of murine brain quantified via diffusion tensor MRI and deformation-based morphometry," *Proceedings of the National Academy of Sciences* 102 (19), 6978-6983 (2005).